Electronic Supplementary Material (ESI) for Nanoscale.

Supporting Information

Multi-wavelength excitable mid-infrared luminescence and energy transfer in core-shell nanoparticles for nanophotonics

Wang Sheng, Jinshu Huang, Zhiyuan Cai, Li He and Bo Zhou*

State Key Laboratory of Luminescent Materials and Devices, Guangdong Provincial Key Laboratory of Fiber Laser Materials and Applied Techniques, Guangdong Engineering Technology Research and Development Center of Special Optical Fiber Materials and Devices, South China University of Technology, Guangzhou 510641, China.

*E-mail: zhoubo@scut.edu.cn

Supporting Figures 1-17

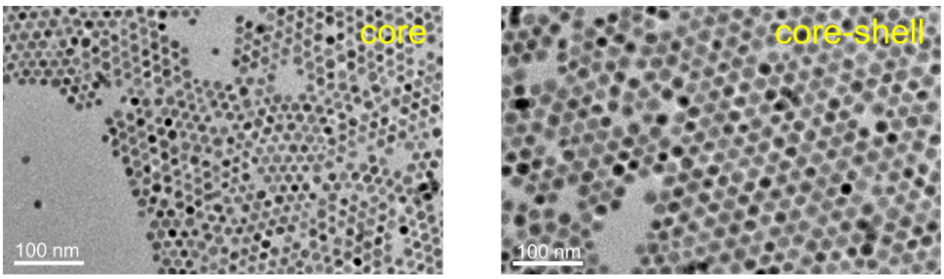

Figure S1. TEM images of the as-synthesized $NaErF_4$:Ho(10 mol%) core (left) and $NaErF_4$:Ho(10 mol%)@$NaYF_4$ core-shell (right) nanoparticles.

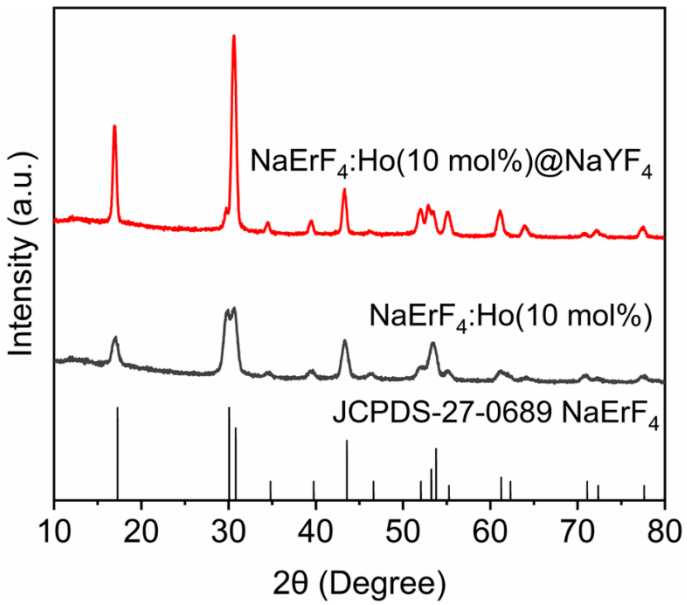

Figure S2. XRD patterns of $NaErF_4$:Ho(10 mol%) core and $NaErF_4$:Ho(10 mol%)@$NaYF_4$ core-shell nanoparticles. The card JCPDS 27-0689 is from hexagonal phase $NaErF_4$.

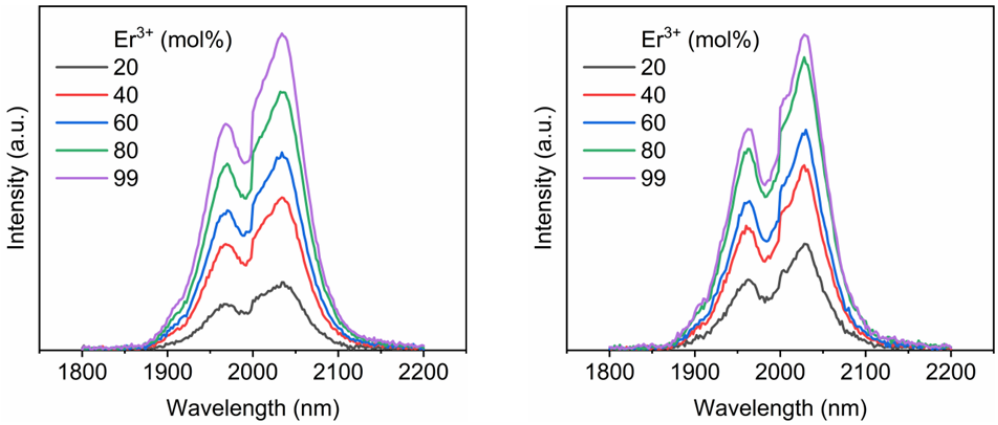

Figure S3. Mid-infrared emission spectra of $NaYF_4$:Er/Ho(20-99/1 mol%)@$NaYF_4$ core-shell nanoparticles under 808 nm (left) and 980 nm (right) excitation, respectively.

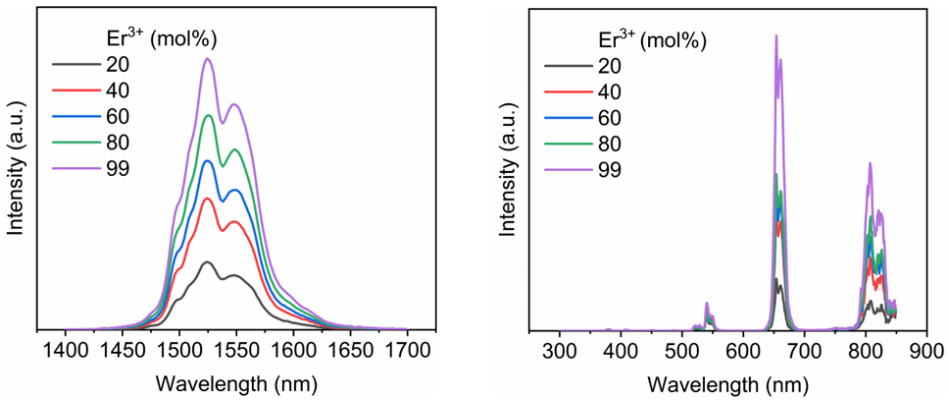

Figure S4. Near-infrared (left) and upconverted (right) emission spectra of $NaYF_4$:Er/Ho(20-99/1 mol%)@$NaYF_4$ core-shell nanoparticles under 980 nm excitation, respectively.

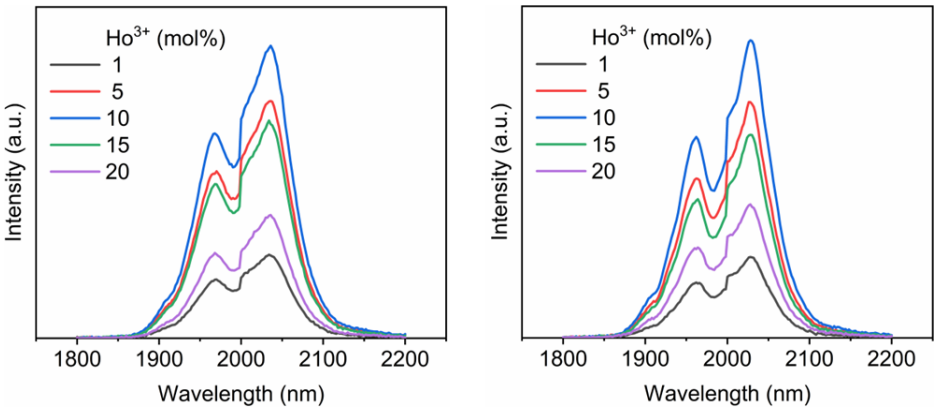

Figure S5. Mid-infrared emission spectra of $NaErF_4$:Ho(1-20 mol%)@$NaYF_4$ core-shell nanoparticles under 808 nm (left) and 980 nm (right) excitations, respectively.

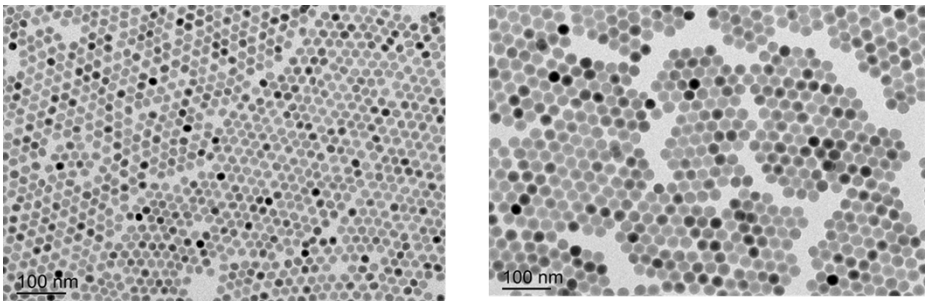

Figure S6. TEM images of the as-synthesized $NaYF_4$:Yb/Ho(20/2 mol%) core (left) and $NaYF_4$:Yb/Ho(20/2 mol%) core-shell (right) nanoparticles.

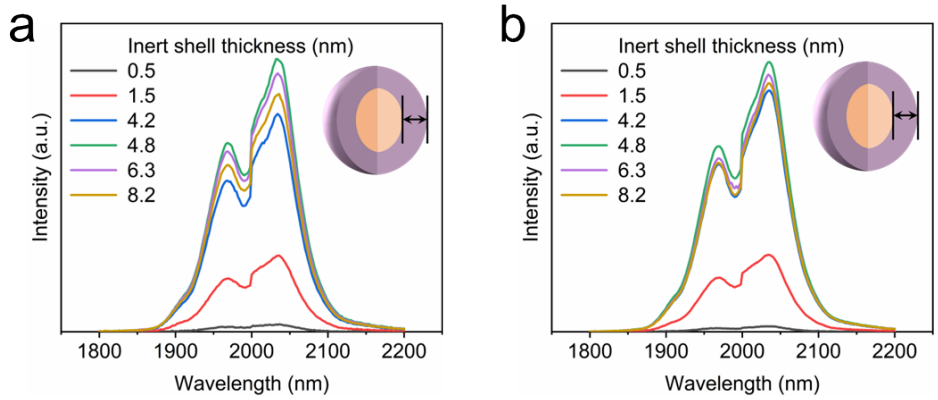

Figure S7. Mid-infrared emission spectra of $NaErF_4$:Ho(10 mol%)@$NaYF_4$ core-shell nanoparticles with various inert shell thicknesses under 808 nm (a) and 980 nm (b) excitations, respectively.

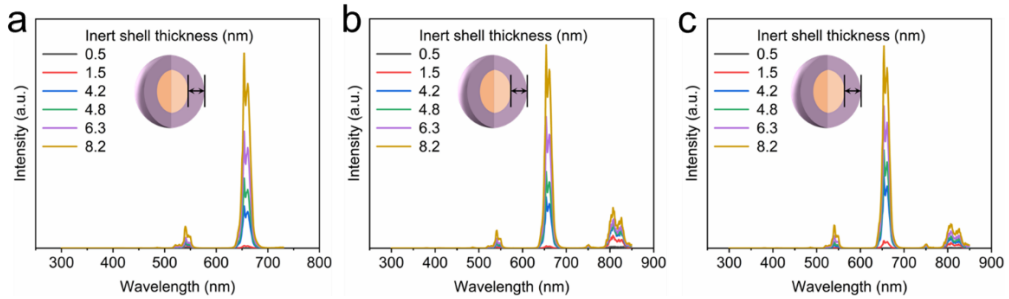

Figure S8. Upconversion emission spectra of $NaErF_4$:Ho(10 mol%)@$NaYF_4$ core-shell nanoparticles with various inert shell thicknesses under 808 nm (a), 980 nm (b) and 1530 nm excitations, respectively.

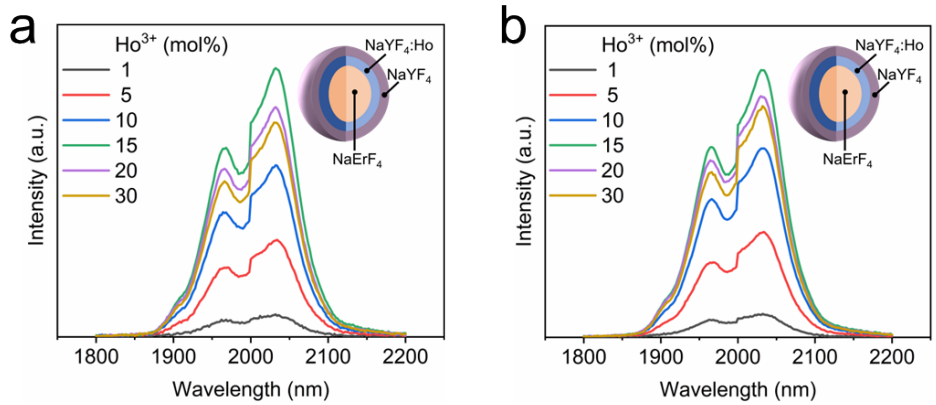

Figure S9. Mid-infrared emission spectra of $NaErF_4$@$NaYF_4$:Ho(1-30 mol%)@$NaYF_4$ samples under 808 nm (a) and 980 nm (b) excitations, respectively.

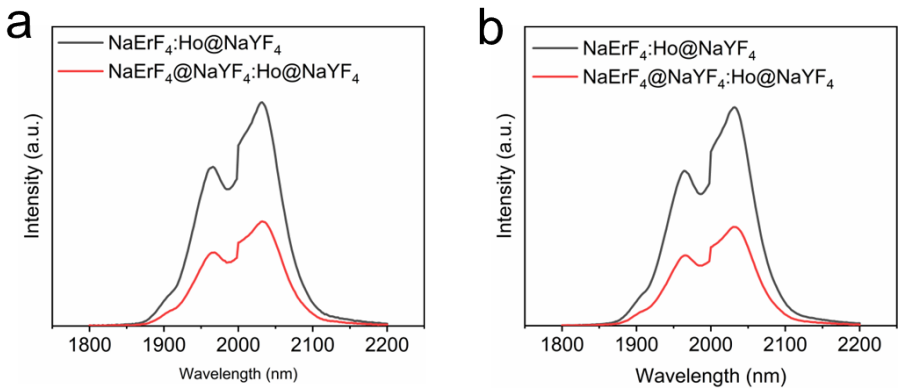

Figure S10. Comparative mid-infrared emission spectra of $NaErF_4$:Ho(10 mol%)@$NaYF_4$ and $NaErF_4$@$NaYF_4$:Ho(15 mol%)@$NaYF_4$ samples under 808 nm (a) and 980 nm (b) excitations, respectively.

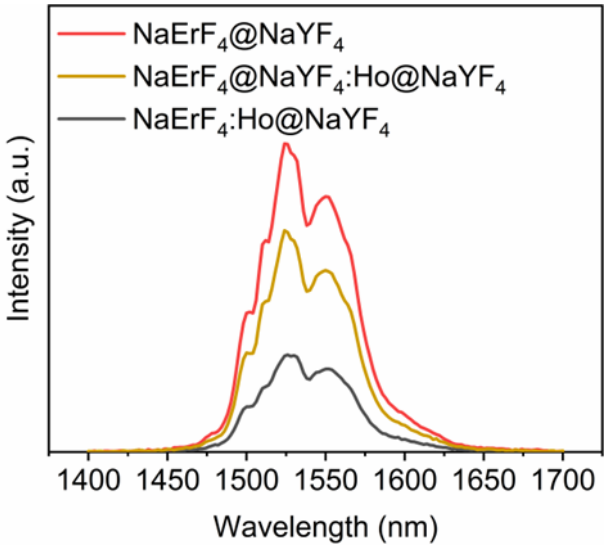

Figure S11. Comparative near-infrared emission spectra of $NaErF_4$@$NaYF_4$, $NaErF_4$@$NaYF_4$:Ho(15 mol%)@$NaYF_4$ and $NaErF_4$:Ho(10 mol%)@$NaYF_4$ samples under 980 nm excitation.

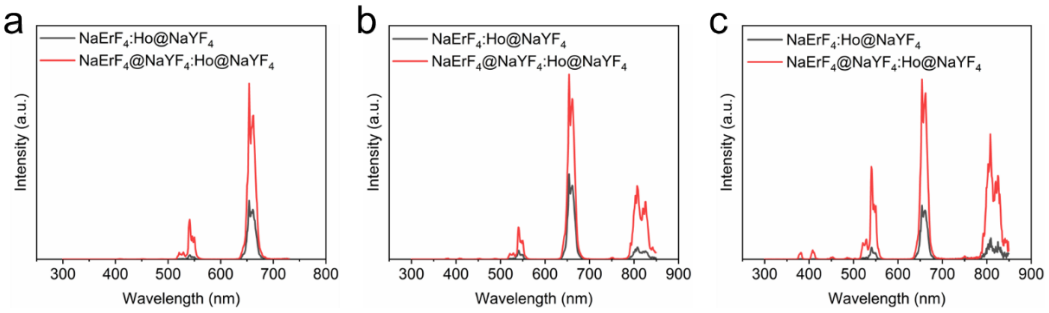

Figure S12. Comparative upconversion emission spectra of $NaErF_4$@$NaYF_4$:Ho(15 mol%)@$NaYF_4$ and $NaErF_4$:Ho(10 mol%)@$NaYF_4$ samples under 808 nm (a), 980 nm (b) and 1530 nm (c) excitations, respectively.

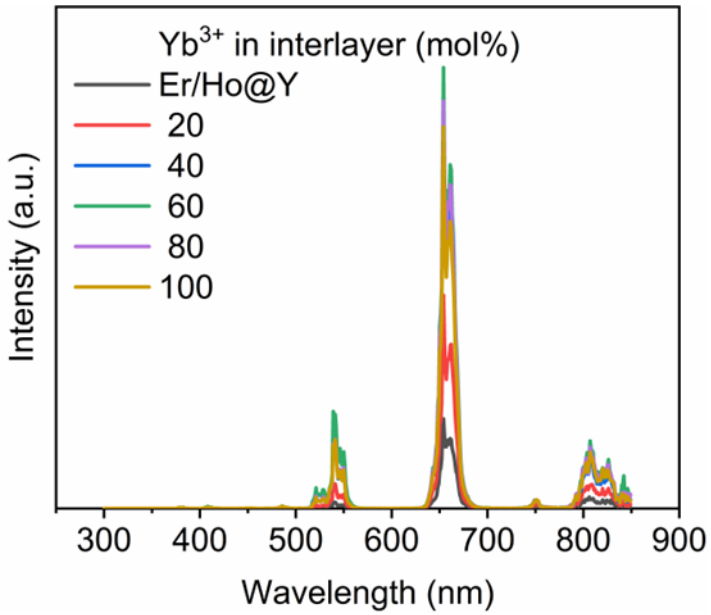

Figure S13. Upconversion emission spectra of $NaErF_4$:Ho(10 mol%)@$NaYF_4$:Yb (20-100 mol%)@$NaYF_4$ core-shell-shell nanoparticles under 980 nm excitation.

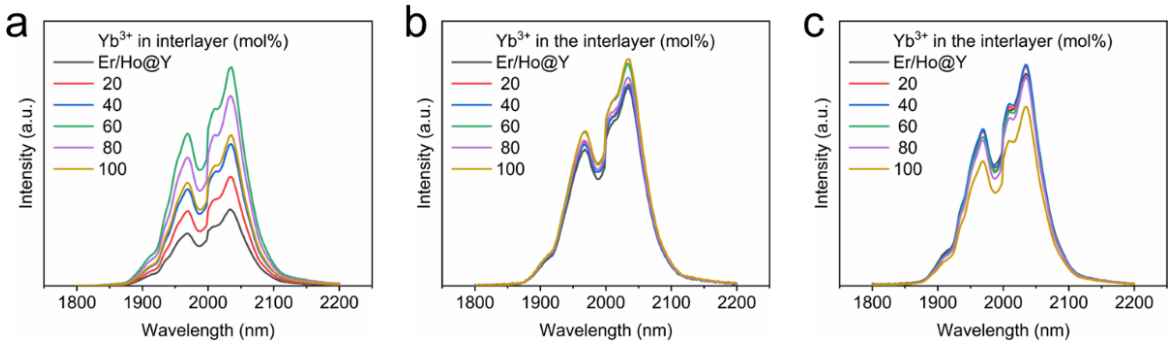

Figure S14. Mid-infrared emission spectra of $NaErF_4$:Ho(10 mol%)@$NaYF_4$:Yb(20-100mol%)@NaYF4 core-shell-shell nanoparticles under 980 nm (a), 808 nm (b) and 1550 nm (c) excitations, respectively.

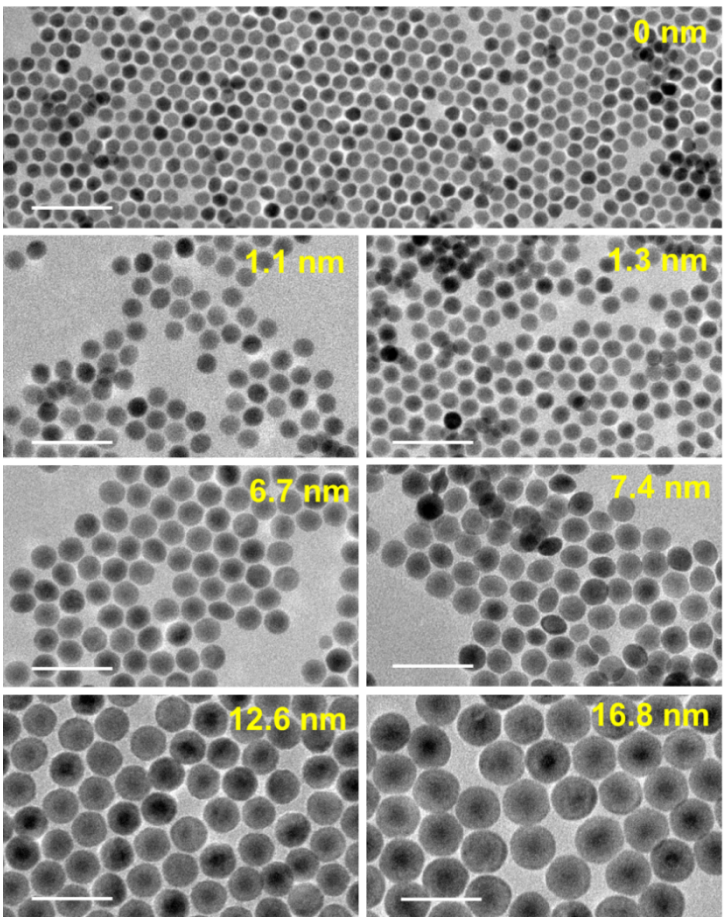

Figure S15. TEM images of the $NaErF_4$:Ho(10 mol%)@$NaYF_4$:Yb(60 mol%) core-shell nanoparticles with different Yb shell thicknesses. $NaYF_4$ inert shell was subsequently coated. The scale bar is 100 nm.

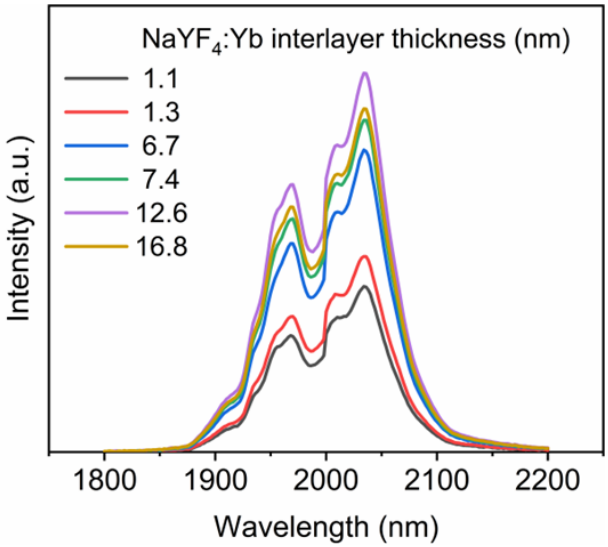

Figure S16. Mid-infrared emission spectra of $NaErF_4$:Ho(10 mol%)@$NaYF_4$:Yb(60 mol%)@$NaYF_4$ core-shell-shell nanoparticles with various interlayer shell thicknesses under 980 nm excitation.

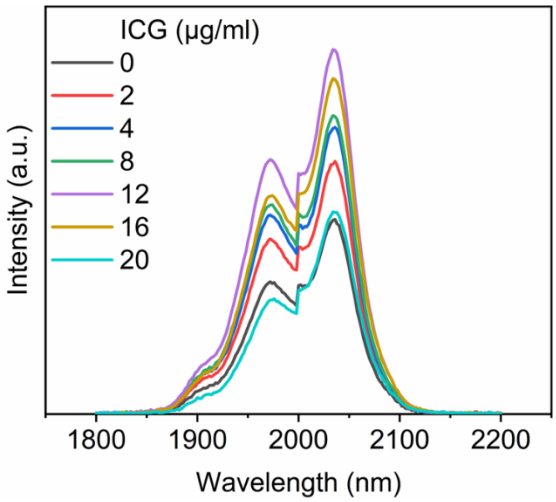

Figure S17. Mid-infrared emission spectra of $NaErF_4$:Ho/Yb(10/10 mol%)@$NaYF_4$:Yb(60 mol%)@$NaYF_4$:Nd/Yb(30/20 mol%) core-shell-shell nanocrystals after modifying with different concentrations of ICG dyes. The excitation wavelength is 808 nm.